ISSN 0036-0244, Russian Journal of Physical Chemistry A, 2019, Vol. 93, No. 8, pp. 1620–1626. © Pleiades Publishing, Ltd., 2019.

PHOTOCHEMISTRY AND MAGNETOCHEMISTRY

TiO_2 Assisted Photocatalytic Decomposition of 2-Chloronaphthalene on Iron Nanoparticles in Aqueous Systems: Synergistic Effect and Intermediate Products

Jipeng Qi[a],*, Chen Wang[a],, Jing Sun[a], and Shuping Li[a]**

[a] School of Environmental Science and Engineering, Qilu University of Technology (Shandong Academy of Science), Jinan, 250353 China

*e-mail: hjqijipeng@163.com

**e-mail: shanqing123@126.com

Received July 9, 2018; revised September 19, 2018; accepted September 21, 2018

Abstract—2-Chloronaphthalene (2-CN), used as an intermediate for organic synthesis, is a new type of persistent organic pollutant. In this work, the decomposition efficiency and decomposition mechanism of 2-CN by zero-valent iron (ZVI) assisted TiO_2 photodecomposition were studied in aqueous medium. Under UV light intensity of 38 mW cm^{-2}, the optimal conditions for photodecomposition at an initial concentration of 5 μmol L^{-1} of 2-CN were pH 3 and 0.04 g L^{-1} TiO_2 and ZVI, as catalysts. Then, the decomposition efficiency of 2-CN reached 66 and 100% in the UV/TiO_2 and UV/ZVI/TiO_2 systems, respectively. Based on analysis of the primary intermediate products of 2-CN, the chlorine on 2-CN was first replaced by a hydroxyl group to form 2-hydroxynaphthalene, and then the naphthalene ring was opened and gradually demethylated to produce small molecules, such as water and carbon dioxide.

Keywords: 2-chloronaphthalene, zero-valent iron, photodecomposition processes, intermediate products, photodecomposition mechanism

DOI: 10.1134/S0036024419080119

INTRODUCTION

In recent years, environmental pollution levels and the distribution characteristics of polychlorinated naphthalenes (PCNs) have attracted widespread attention [1–3]. PCNs have been identified in air, water, soil, sediment and biological matrices [4–8]. Although environmental concentrations are typically as low as ng L^{-1} or μg L^{-1}, PCNs may deteriorate the health of humans and aquatic species, due to bioaccumulation, toxicity, and lipophilic physico-chemical properties [9–12]. Long-term exposure to PCNs can damage organs, causing chloracene and liver disease [13]. 2-CN can be used as a model compound in studying the processes involving more toxic PCNs. The decomposition of 2-CN in water and wastewater has not been evaluated in previous studies.

In the past few decades, advanced oxidation processes have been applied to the decomposition of organic contaminants [14, 15]. Many of these methods are based on the formation of highly reactive hydroxyl radicals (OH). As a result of high oxidation potential, OH can degradation organic contaminants into intermediate compounds and even dissolve them in water, carbon dioxide, and other inorganic compounds [16, 17]. Photocatalytic degradation has been suggested as an attractive way to treat contaminated wastewater, since it is cost-effective and non-toxic [18–20]. Various catalysts have been applied during heterogeneous photocatalysis, such as TiO_2, ZnO, ZnS, Fe_2O_3, and MnO_2. Among them, TiO_2 was the most effective, due to long-term stability, controllable structure and economic excellence [21, 22]. However, TiO_2 has poor visible light absorption and relatively rapid recombination of charge carriers, limiting photocatalytic activity [23]. Specifically, the photocatalytic electron–hole pairs of TiO_2 have flash recombination on the order of 10^{-9} s, which is much shorter than the chemical interaction time of TiO_2 with adsorbed pollutants [24].

ZVI, one of the most widely used zero-valent metals, is readily available, inexpensive, and non-toxic [25]. Recently, ZVI was combined with photocatalytic and considered to be a novel reactive method to enhance the photoreaction efficiency of TiO_2 [26]. ZVI can completely decompose and dissolve harmful organic contaminants [27]. The major mechanisms enhanced by ZVI include (a) inhibition of electron–hole pair recombination in TiO_2 and (b) production of ferrous ions in acidic conditions, which could form Fenton-like system with hydroxyl radicals [28].

This study investigated the decomposition of 2-CN using the UV/ZVI/TiO_2 system. The effects of operating parameters, including light source, light intensity, catalyst concentration, pH, and initial concentration of 2-CN on the photocatalytic decomposition, were investigated. Finally, the optimal photodecomposition conditions and potential photodecomposition mechanism of 2-CN were studied.

MATERIALS AND METHODS

Chemical Regents

2-CN (98.5%) was obtained from Bailingwei Company (Beijing, China). Acetonitrile, *tert*-butanol and methanol (chromatographic grade) were obtained from Merck (Germany). TiO_2 (Anatase P25, with average particle size of 30 nm, purity >99%) and ZVI (with average particle size of 30 μm, purity >99%) were obtained from Sinopharm Chemical Reagent Co (Shanghai, China). All chemical reagents were of analytical grade. All solutions were prepared using ultrapure water from a Millipore water purification system.

Analysis Procedures

2-CN was measured using a high-performance liquid chromatography (HPLC) (LC-20A, Shimadzu, Japan) equipped with a C18 reverse phase column (dimensions: 250 × 4.6 mm, 5 μm) and a UV detector set at 225 nm. The mobile phase was a mixture of water and acetonitrile (vol/vol = 20 : 80) at a flow rate of 1.0 mL min^{-1}. The temperature of the column was maintained at 30°C. The oxidation by-products were identified by liquid chromatography mass spectrometry (HPLC-MS/8040, Shimadzu, Japan), equipped with Triple Quad MS, using ESI-ionization and operating in full-scan mode. Separation was carried out using a C18 column (dimensions: 4.6 × 250 mm, 5 μm) at a flow rate of 0.5 mL min^{-1}. The mobile phase was a mixture of acetonitrile and purified water (vol/vol = 80 : 20). Chlorine ions produced from 2-CN decomposition were identified by ionic chromatography (IC 90, Dionex, USA) equipped with a column Dionex IonPac ASC14 (250 × 4.0 mm) and a conductivity detector. The eluent was mixed with 3.5 mM $NaCO_3$ and 1.0 mM $NaHCO_3$ at a flow rate of 1.0 mL min^{-1}.

Experimental Procedures

All experiments were conducted in a 500-mL capacity bath photoreactor (Xujiang, Nanjing, China). Three light sources were used: a UV lamp, a Xe lamp and sunlight. A cooling system was also installed in the reactor to maintain the experimental temperature at 25 ± 1°C.

A 500 μmol L^{-1} stock solution of 2-CN was prepared in an amber bottle. To investigate the effect of the initial 2-CN concentration, concentrations of 2-CN from 5 to 40 μmol L^{-1} were used. Then, 5 μmol L^{-1} of 2-CN was used in other experiments, unless otherwise stated. Different concentrations of TiO_2 or ZVI were mixed with 2-CN solution at pH 3 in the UV/TiO_2 and UV/ZVI/TiO_2 systems, respectively. To study the effect of pH on 2-CN decomposition, the required amounts of NaOH or H_2SO_4 were added to the samples to obtain the desired solution pH. The suspensions were stirred magnetically for the dark adsorption experiment. Before irradiation, the photoreactor was kept in the dark for 60 min to achieve adsorption equilibrium. All samples were treated in triplicate.

RESULTS AND DISCUSSION

Effect of Light Source and Irradiation Intensity

The light source and irradiation intensity have been reported to be crucial parameters influencing the direct photodecomposition of pollutants [29]. In this study, the decomposition of 2-CN was investigated under various light sources (i.e., UV lamp, Xe lamp, and sunlight) and at different intensities of UV lamps (i.e., 20, 32, and 38 mW cm^{-2}). The initial 2-CN concentration was 5 μmol L^{-1}, and the initial pH value of the solution was 7.0. Figure 1a demonstrates the decomposition efficiency of 2-CN under irradiation by different light sources. 2-CN was slightly decomposed by the sunlight irradiation process. The decomposition efficiency of 2-CN was only 8.0% after 480 min of sunlight irradiation. This result revealed that 2-CN persists in the environment, with limited degradation. The decomposition efficiency of 2-CN was 24.0% after Xe lamp irradiation for 480 min. When 2-CN was exposed to UV irradiation alone, the decomposition efficiency of 2-CN was promoted to 32.0% after 120 min. The photodecomposition reaction under sunlight irradiation proceeded slowest. The 2-CN photolysis efficiency was much higher under UV light than under the Xe lamp. These results revealed that UV radiation was very effective for 2-CN photodecomposition.

The 2-CN spectrum was characterized by an ultraviolet spectrophotometer, at 225 nm. In this study, UV light irradiation was provided by a 300-W medium-pressure mercury lamp (366 nm). 2-CN may not be able to undergo direct photolysis, and water molecules likely produce active radicals under UV light irradiation. Therefore, 2-CN is oxidized by active species under UV irradiation. As a typical radical quencher, tertiary butanol (*t*-BuOH) can react with active species during UV irradiation [30]. Therefore *t*-BuOH was used to investigate the effect of active species on 2-CN decomposition during direct UV irradiation processes. Specifically, with the injection of *t*-BuOH from 1.0 to 5.0 mL, the decomposition efficiency of

2-CN decreased from 32.0 to 12.0% after 120 min. This indicated that water molecules may produce active species under UV irradiation.

Figure 1b shows the decomposition efficiency of 2-CN under various irradiation intensities. The decomposition efficiency of 2-CN slightly increased with increasing irradiation intensity. The decomposition efficiency of 2-CN increased from 32.0 to 41.0% when the irradiation intensity of UV lamp increased from 20 to 38 mW cm^{-2}. Therefore, the decomposition efficiency of 2-CN increased with the light intensity. This phenomenon indicated that high photon flux increased the probability of collision between photons and activated sites on 2-CN, which enhanced the rate of photolysis reaction [31]. To improve the decomposition efficiency of 2-CN, light intensity of 38 mW cm^{-2} was applied to the following experiments.

Effect of Catalyst Concentration

TiO_2 is a widely used photocatalyst because of high catalytic activity, and the concentration of TiO_2 affected the generation of hydroxyl radicals during photodecomposition process. ZVI is oxidized to ferrous ions in aqueous solution under acidic conditions, which can generate a Fenton-like system with hydroxyl radicals [28]. This study determined the optimal concentration of TiO_2, and then added different concentrations of ZVI. Finally, the optimal concentration of ZVI was determined to generate the UV/ZVI/TiO_2 system. Before irradiation, the reaction mixture of the catalyst and 2-CN was stirred in darkness to achieve adsorption equilibrium. The adsorption capacity was gradually increased and stabilized with time. The maximum adsorption of TiO_2 and ZVI was 8.0, 6.0, and 13.0%, respectively (Fig. 2a). The effects of the concentration of TiO_2 (0–0.08 g L^{-1}) (Fig. 2b) and ZVI (0–0.06 g L^{-1}) (Fig. 2c) on the decomposition of 2-CN was investigated with an initial 2-CN concentration of 5 μmol L^{-1} at pH 3.0, with a medium-pressure mercury lamp and an irradiation time of 60 min.

In the UV/TiO_2 system, the decomposition efficiency of 2-CN increased from 41.0 to 66.0% with increasing TiO_2 concentration from 0 to 0.04 g L^{-1} after 60 min UV irradiation (Fig. 2b), respectively. This was because the water molecule and hydroxyl ions were oxidized to hydroxyl radicals by the surface hole of TiO_2. The concentration of hydroxyl radicals gradually increased with increasing TiO_2, thus enhancing the decomposition efficiency of 2-CN. However, the decomposition efficiency of 2-CN decreased from 66.0 to 56.0% with increasing TiO_2 concentration from 0.04 to 0.08 g L^{-1} after 60 min UV irradiation. Above 0.04 g L^{-1} of TiO_2, the decomposition efficiency of 2-CN gradually decreased. Increased TiO_2 concentration likely resulted in the absorption of some photons. A higher concentration of TiO_2 further produced a screening effect for UV light irradiation [32, 33], reducing the decomposition efficiency of 2-CN. Therefore, the optimal concentration of TiO_2 for the decomposition of 2-CN was 0.04 g L^{-1}.

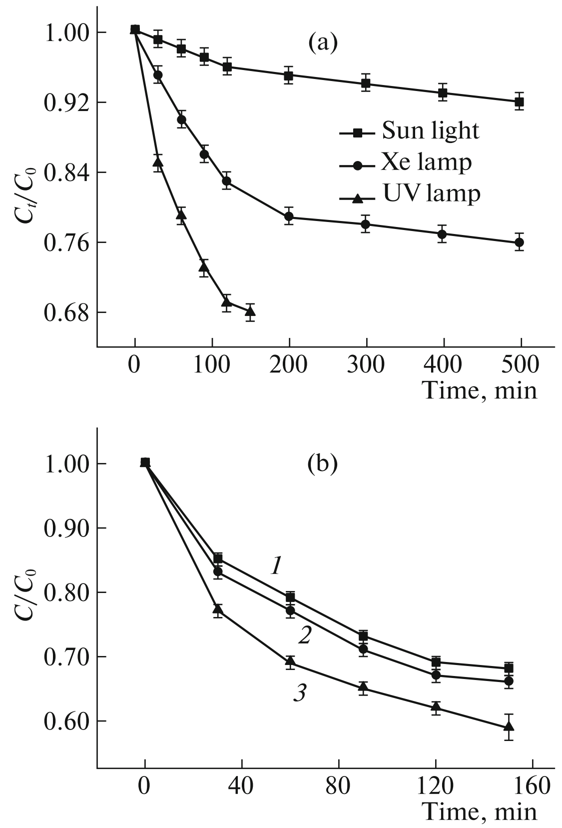

Fig. 1. Effect of light source (a) and irradiation intensity (b) on decomposition of 2-CN; 5 μmol L^{-1} of 2-CN, pH 7, without TiO_2 or ZVI; *1*—20, *2*—32, *3*—38 mW cm^{-2}.

Figures 2c, 2d demonstrate the effect of ZVI concentration on the decomposition of 2-CN at pH 3.0 in the UV/ZVI and UV/ZVI/TiO_2 systems, respectively. As shown in Fig. 2c, the decomposition efficiency increased slowly from 41.0 to 47.0% as the addition of ZVI changed from 0 to 0.06 g L^{-1} in the UV/ZVI system. As shown in Fig. 2d, the decomposition efficiency increased rapidly from 66.0 to 100% as the addition of ZVI changed from 0 to 0.04 g L^{-1} in the UV/ZVI/TiO_2 system. The major mechanisms enhanced by ZVI include (a) inhibition of electron—hole pair recombination in TiO_2 and (b) production of ferrous ions in acidic conditions, which could form Fenton-like system with hydroxyl radicals. However, higher concentrations of ZVI did not improve the decomposition efficiency of 2-CN: with increased concentration of ZVI from 0.04 to 0.06 g L^{-1}, the efficiency of 2-CN was decreased. Decreased decomposi-

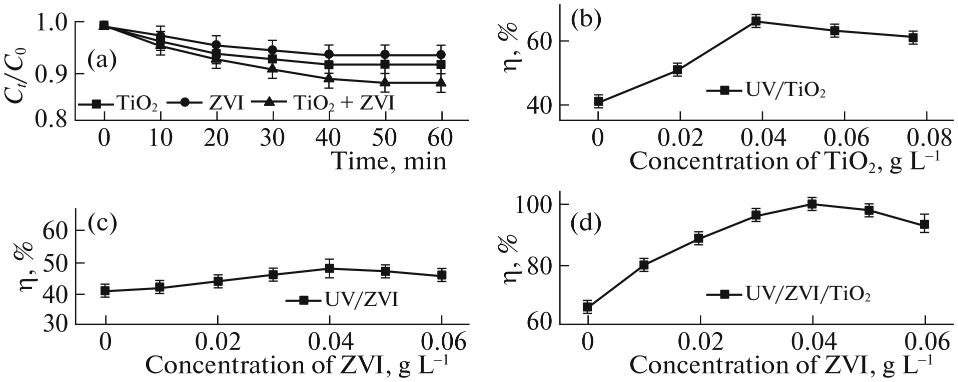

Fig. 2. Effect of TiO_2 and ZVI concentration on the photodecomposition efficiency(η) of 2-CN; concentration of 2-CN was 5 μmol L^{-1}, pH 3.0; concentration of TiO_2: (a) 0.08, (b, c) from 0 to 0.08, (d) 0.04 g L^{-1}; concentration of ZVI: (a) 0.06, (b) 0, (c) from 0 to 0.06, (d) 0.04 g L^{-1}.

tion efficiency of 2-CN at high ZVI concentrations may result from particle screening, as the generated hydroxyl radical is scavenged by the iron surface. Miller reported that the hydroxyl radical was very reactive with iron oxide [34]. High reactivity between the iron and hydroxyl radical may reduce the decomposition of 2-CN. Therefore, the most effective concentration of ZVI for the decomposition of 2-CN was 0.04 g L^{-1}.

Effect of pH

The effect of pH on the photodecomposition of 2-CN was investigated over the pH range of 3.0–9.0 with an initial concentration of 5 μmol L^{-1} 2-CN, 0.04 g L^{-1} TiO_2, 0.04 g L^{-1} ZVI, light intensity of 38 mW cm^{-2}, and irradiation time of 60 min.

Figure 3 shows that the decomposition efficiency of 2-CN decreased from 100 to 25.0% with increased pH from 3.0 to 9.0 in the UV/ZVI/TiO_2 system after 60 min UV irradiation. Apparently, the decomposition efficiency of 2-CN was faster in acidic solutions than in alkaline solutions in the UV/ZVI/TiO_2 system. Because the point of zero charge (PZC) of TiO_2 was 6.3, when the initial solution pH was below the PZC of TiO_2, the surface of TiO_2 was positively charged. This enabled it to absorb negatively charged 2-CN molecules, enhancing the decomposition efficiency of 2-CN. Conversely, when the pH was above PZC, the surfaces of both TiO_2 and 2-CN were negatively charged, resulting in electrostatic repulsion and reducing the decomposition efficiency of 2-CN. Under acidic conditions, oxygen molecules were reduced by electrons (e^-) on the surface of TiO_2 to produce superoxide radicals ($O_2^{\bullet-}$). Superoxide radicals promoted the formation of hydrogen peroxide by following reactions [35]:

$$e^- + O_2 \rightarrow O_2^{\bullet-}, \quad (1)$$

$$O_2^{\bullet-} + H^+ \rightarrow HO_2^{\bullet}, \quad (2)$$

$$HO_2^{\bullet} + H^+ + e^- \rightarrow H_2O_2, \quad (3)$$

which had stronger oxidation susceptibility. At pH values greater than 5.0 and 7.0, the decomposition efficiency of 2-CN was decreased due to the following processes: (a) the scavenging of $^{\bullet}OH$ by H^+ ions and (b) more Fe^{2+} formed precipitates and lost catalytic ability. These results demonstrated that the UV/ZVI/TiO_2 system was more effective for the oxidation decomposition of 2-CN under acidic conditions. Therefore, the optimal pH value for the decomposition of 2-CN in the UV/ZVI/TiO_2 system was 3.0.

Effect of Radical Scavengers

To better understand the properties of active radicals in the decomposition of 2-CN, radical scavenger experiments were carried out in the UV/ZVI/TiO_2 system. Isopropanol was used as a scavenger, because it can react with hydroxyl radicals. EDTA-2Na was also used as a scavenger, because it could react with H^+. Finally, since *p*-benzoquinone could react with superoxide radicals, it was also used as a scavenger [36].

As shown in Fig. 4, the decomposition efficiency of 2-CN decreased from 100 to 62.0, 75.0, and 80.0% with the addition of isopropanol, *p*-benzoquinone and EDTA-2Na, respectively. These results indicated that HO/O_2^- radicals played an important role in 2-CN decomposition in the UV/ZVI/TiO_2 system. H^+ also could promote the decomposition of 2-CN in the UV/ZVI/TiO_2 system. This phenomenon could be associated with efficient photogenerated electron

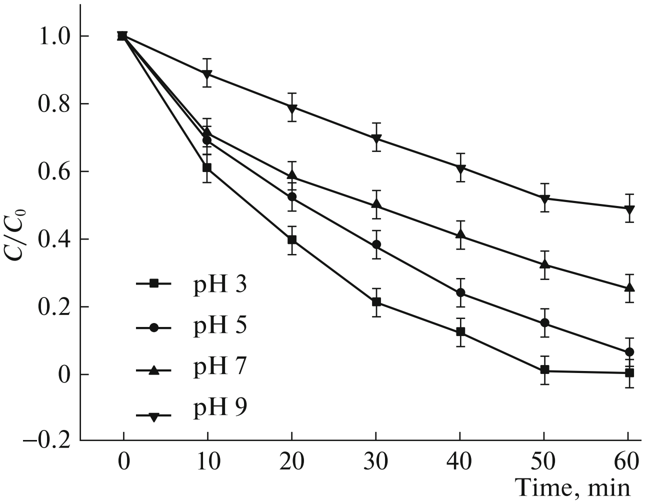

Fig. 3. Effect of pH on decomposition of 2-CN in $UV/ZVI/TiO_2$ system (concentration of 2-CN was 5 μmol L^{-1}, concentration of TiO_2 was 0.04 g L^{-1}, and concentration of ZVI was 0.04 g L^{-1}, with pH from 3.0 to 9.0).

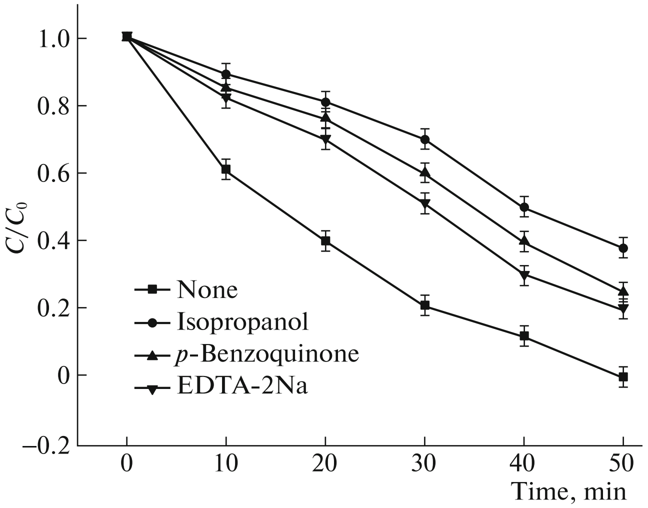

Fig. 4. Effect of isopropanol, *p*-benzoquinone, and EDTA-2Na on the decomposition of 2-CN (concentration of 2-CN was 5.0 μmol L^{-1}, pH 3, concentration of TiO_2 was 0.04 g L^{-1}, and concentration of ZVI was 0.04 g L^{-1}).

transfer in the $UV/ZVI/TiO_2$ system, which facilitated greater participation by H^+ in the photocatalytic processes and greatly promoted oxygen molecules to yield superoxide radicals [37, 38]. These superoxide radicals further induced the formation of H_2O_2 and then participated in the photocatalytic processes. Therefore, HO/O_2^- radicals contributed more to the decomposition of 2-CN.

Effect of 2-CN Initial Concentration and Kinetics Analysis

The effect of the initial concentration of 2-CN on the photodecomposition efficiency was investigated over a concentration range from 5.0 to 40.0 μmol L^{-1}. Figure 5a demonstrates the decomposition of 2-CN under various initial concentrations. The decomposition efficiency of 2-CN was decreased from 100 to 79.0% as the concentration of 2-CN increased from 5.0 to 40.0 μmol L^{-1} after 60 min in the $UV/ZVI/TiO_2$ system. The decreased decomposition efficiency in the $UV/ZVI/TiO_2$ system was mainly caused by the following processes: (a) some hydroxyl radicals could be captured by the intermediate products of 2-CN, and (b) the same concentration of catalyst generated stable amounts of hydroxyl radicals, which were not sufficient for the oxidation of the 2-CN at higher 2-CN concentrations.

The initial concentration crucially affected the decomposition kinetics. The pseudo-first-order kinetic rate constants for 2-CN decomposition at different initial concentrations are listed in Table 1. In this study, the removal of 2-CN was fit with the pseudo-first-order reaction kinetics model (Fig. 5b). The decomposition rate constants, (k, min^{-1}), of 2-CN decreased with increased initial concentration, and the pseudo-first-order rate constant k decreased from 0.050 to 0.023 min^{-1}. The results demonstrated that the initial concentration greatly affected the decomposition rate of 2-CN.

Identification of Intermediate Products

In this study, the intermediate products of 2-CN were detected by HPLC-MS under the optimal photodecomposition conditions for 2-CN. The decomposition solutions of 2-CN were collected in the UV/TiO_2 and $UV/ZVI/TiO_2$ system at the irradiation times of 10, 20, 30, 40, and 50 min. Then, 10 μL of each sample solution was injected into the HPLC-MS system. Four intermediate products were detected in both the UV/TiO_2 and $UV/ZVI/TiO_2$ systems, which indicated that the photodecomposition of 2-CN had a similar pathway in both systems. When the irradiation time reached 10 min, the most abundant fragment, ion

Table 1. Pseudo-first-order kinetics for 2-CN decomposition at different initial concentrations (C_0), R^2 is correlation coefficient

C_0, μmol L^{-1}	Decomposition, %	k, min^{-1}	R^2
5	100 (50 min)	0.050	0.993
10	99 (60 min)	0.048	0.920
20	95 (60 min)	0.036	0.913
40	79 (60 min)	0.023	0.975

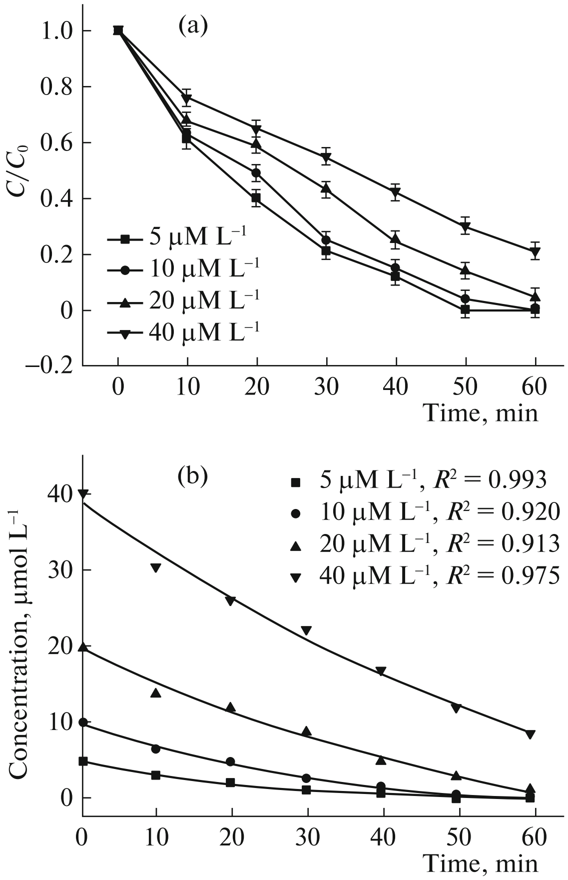

Fig. 5. Effect of initial concentration on decomposition of 2-CN (concentration of 2-CN was 5.0 to 40 μmol L^{-1}, pH 3, concentration of TiO$_2$ was 0.04 g L^{-1}, and concentration of ZVI was 0.04 g L^{-1}; (a) decomposition efficiency of 2-CN; (b) kinetic model decomposition of 2-CN.

m/z = 144, was obtained. The ion at m/z = 144 was identified as naphthol. When the irradiation time reached 20 min, the most abundant fragment was ion m/z = 129, identified as naphthalene. When the irradiation time reached 30 min, the most abundant fragment, m/z = 105, was obtained, which was identified as ethylbenzene. When the irradiation time reached 40 min, the most abundant fragment was m/z = 69, pentyne. When the irradiation time reached 50 min, the primary intermediate products of 2-CN remained unchanged, and the decomposition efficiency of 2-CN reached 100%. These results indicated that the primary intermediate products of 2-CN were naphthol, naphthalene, ethylbenzene, and pentyne. These results also support the efficiency of the UV/ZVI/TiO$_2$ system for the photodecomposition of 2-CN.

Combining an understanding of the generated ions with the identification results of the intermediate products, a possible decomposition pathway of 2-CN was proposed, as shown in Fig. 6: 2-CN was first attacked by OH to release chloride and form naphthol. Then, the naphthalene ring was broken by OH oxidation to form alkyne and ethyl. Finally, the intermediate products of 2-CN were further decomposed into H_2O and CO_2.

CONCLUSIONS

In this study, the optimal photodecomposition conditions and photodecomposition mechanism of 2-CN were determined. ZVI enhanced the oxidation susceptibility of the UV/TiO$_2$ system. The decomposition of 2-CN followed the pseudo-first-order kinetic model. The intermediate products of 2-CN were pri-

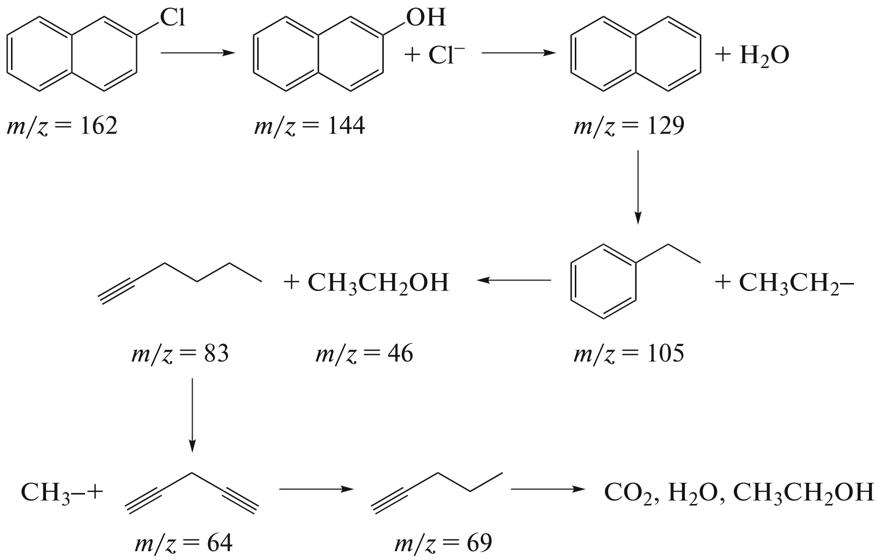

Fig. 6. Decomposition pathway for photodecomposition of 2-CN (concentration of 2-CN was 5.0 μmol L^{-1}, pH 3.0, concentration of TiO$_2$ was 0.04 g L^{-1}, and concentration of ZVI was 0.04 g L^{-1}).

marily naphthol, naphthalene, ethylbenzene, and pentyne. From the analysis of the primary intermediate products of 2-CN, the chlorine atom on 2-CN was first replaced by a hydroxyl group to form 2-hydroxynaphthalene, and then the naphthalene ring was opened and gradually demethylated to produce small molecules, such as ethanol.

ACKNOWLEDGMENTS

The authors thank the staff of Key Laboratory of Cleaner Production and Industrial Wastes Recycling and Resourcization in Universities of Shandong, Qilu University of Technology (Shandong Academy of Science). This work was supported by the National Nature Science Foundation of China (no. 21507067).

REFERENCES

1. L. Guo, T. Ba, and M. H. Zheng, Prog. Chem. **29**, 377 (2009).
2. Y. Xu, J. Li, P. Chakraborty, J. H. Syed, R. N. Malik, Y. Wang, C. Tian, C. Luo, G. Zhang, and K. C. Jones, Sci. Total Environ. **466–467,** 1030 (2014).
3. L. Xue, L. Zhang, Y. Yan, L. Dong, Y. Huang, and X. Li, Chemosphere **162**, 199 (2016).
4. Q. Die, Z. Nie, Y. Fang, Y. Yang, X. Gao, Y. Tian, J. He, F. Liu, Q. Huang, and S. Tian, Chemosphere **144**, 2134 (2016).
5. H. Zhang, K. Xiao, J. Liu, T. Wang, G. Liu, Y. Wang, and G. Jiang, Sci. Total Environ. **490**, 555 (2014).
6. F. Li, J. Jin, Y. Gao, N. Geng, D. Tan, H. Zhang, Y. Ni, and J. Chen, Environ. Pollut. **211**, 226 (2016).
7. Y. Wang, Z. Cheng, J. Li, C. Luo, Y. Xu, Q. Li, X. Liu, and G. Zhang, Environ. Pollut. **170**, 1 (2012).
8. L. Zhang, L. Zhang, L. Dong, Y. Huang, and X. Li, Chemosphere **138**, 668 (2015).
9. Q. Zhu, X. Zhang, S. Dong, L. Gao, G. Liu, and M. Zheng, Environ. Pollut. **212**, 128 (2016).
10. S. Corsolini, K. Kannan, T. Imagawa, F. Silvano, and J. Giesy, Marine Food Webs **36**, 3490 (2002).
11. P. A. Behnisch, K. Hosoe and S.-I. Sakai, Environ. Int. **29**, 861 (2003).
12. D. Hayward, Environ. Res. **76**, 1 (1998).
13. D. Villeneuve, K. Kannan, J. S. Khim, J. Falandysz, V. Nikiforov, A. L. Blankenship, and J. Giesy, Arch. Environ. Contamin. Toxicol. **39**, 273 (2000).
14. D. N. Khue, N. V. Chat, D. B. Minh, T. D. Lam, P. H. Lan, and V. D. Loi, Mater. Sci. Eng. C **33**, 1975 (2013).
15. B. A. Wols, D. J. H. Harmsen, E. F. Beerendonk, and C. H. M. Hofman-Caris, Chem. Eng. J. **263**, 336 (2015).
16. D. Hokanson, K. Li, and R. Trussell, Front. Environ. Sci. Eng. **10**, 428 (2016).
17. E. Kan, C. I. Koh, K. Lee, and J. Kang, Front. Environ. Sci. Eng. **9**, 429 (2015).
18. A. Tomašević, E. Kiss, S. Petrović, and D. Mijin, Desalination **262**, 228 (2010).
19. A. Tomašević, D. Mijin, S. Gašić, and E. Kiss, Desalin. Water Treat. **52**, 4342 (2014).
20. A. Sharma and B. K. Lee, J. Environ. Manage. **165**, 1 (2016).
21. N. Daneshvar, D. Salari, and A. R. Khataee, J. Photochem. Photobiol., A **157**, 111 (2003).
22. N. Daneshvar, D. Salari, and A. R. Khataee, J. Photochem. Photobiol., A **162**, 317 (2004).
23. S. Bagheri and N. M. Julkapli, Int. J. Hydrogen Energy **41**, 14652 (2016).
24. M. R. Hoffmann, S. T. Martin, W. Choi, and D. W. Bahnemann, Chem. Rev. **95**, 69 (1995).
25. J. A. Bergendahla and T. P. Thies, Water Res. **38**, 327 (2004).
26. M. Safari, M. Nikazar, and M. Dadvar, J. Ind. Eng. Chem. **19**, 1697 (2013).
27. Z. H. Ai, Z. T. Gao, L. Z. Zhang, W. W. He, and J. J. Yin, Environ. Sci. Technol. **47**, 5344 (2013).
28. A. A. Burbano, D. D. Dionysiou, M. T. Suidan, and T. L. Richardson, Water. Res. **39**, 107 (2005).
29. P. Mazierski, J. Nadolna, W. Lisowski, M. J. Winiarski, M. Gazda, M. Nischk, T. Klimczuk, and A. Zaleska-Medynska, Catal. Today **284**, 19 (2017).
30. N. Huang, T. Wang, W. L. Wang, Q. Y. Wu, A. Li, and H. Y. Hu, Water Res. **114**, 246 (2017).
31. M. Safari, M. Nikazar, and M. Dadvar, J. Ind. Eng. Chem. **19**, 1697 (2013).
32. T. F. Li, T. C. Wang, G. Z. Qu, D. L. Liang, and S. B. Hu, Environ. Sci. Pollut. Res. **24**, 12416 (2017).
33. G. Zhou, J. Guo, X. Wan, and H. Shi, J. Environ. Sci. **47**, 63 (2016); Environ. Sci. Pollut. Res. **24**, 10421 (2017).
34. C. M. Miller and R. L. Valentine, Water Res. **33**, 2805 (1999).
35. M. Safari, M. Nikazar, and M. Dadvar, J. Ind. Eng. Chem. **19**, 1697 (2013).
36. J. Sun, H. Zhang, L. H. Guo, and L. Zhao, ACS Appl. Mater. Interfaces **5**, 13035 (2013).
37. T. Hirakawa and Y. Nosaka, Langmuir **18**, 3247 (2002).
38. N. Zhang, Y. Zhang, X. Pan, M. Q. Yang, and Y. J. Xu, J. Phys. Chem. C **116**, 18023 (2012).